



Comparative Genomics and Transcriptomics During Sexual Development Gives Insight Into the Life History of the Cosmopolitan Fungus *Fusarium neocosmosporiellum*

OPEN ACCESS

Edited by:

Gustavo Henrique Goldman,
University of São Paulo, Brazil

Reviewed by:

Theo Van Der Lee,
Wageningen University & Research,
Netherlands
Thomas Nussbaumer,
Institut für Umweltmedizin (IEM),
Germany

*Correspondence:

Frances Trail
trail@msu.edu

† Present address:

Wonyong Kim,
Korean Lichen Research Institute,
Suncheon National University,
Suncheon, South Korea

Specialty section:

This article was submitted to
Fungi and Their Interactions,
a section of the journal
Frontiers in Microbiology

Received: 17 January 2019

Accepted: 20 May 2019

Published: 07 June 2019

Citation:

Kim W, Cavinder B, Proctor RH,
O'Donnell K, Townsend JP and Trail F
(2019) Comparative Genomics
and Transcriptomics During Sexual
Development Gives Insight Into
the Life History of the Cosmopolitan
Fungus *Fusarium*
neocosmosporiellum.
Front. Microbiol. 10:1247.
doi: 10.3389/fmicb.2019.01247

Wonyong Kim^{1†}, Brad Cavinder¹, Robert H. Proctor², Kerry O'Donnell²,
Jeffrey P. Townsend^{3,4} and Frances Trail^{1,5*}

¹ Department of Plant Biology, Michigan State University, East Lansing, MI, United States, ² Mycotoxin Prevention and Applied Microbiology Research Unit, United States Department of Agriculture, Peoria, IL, United States, ³ Department of Biostatistics, Yale University, New Haven, CT, United States, ⁴ Department of Ecology and Evolutionary Biology, Yale University, New Haven, CT, United States, ⁵ Department of Plant, Soil and Microbial Sciences, Michigan State University, East Lansing, MI, United States

Fusarium neocosmosporiellum (formerly *Neocosmospora vasinfecta*) is a cosmopolitan fungus that has been reported from soil, herbivore dung, and as a fruit- and root-rot pathogen of numerous field crops, although it is not known to cause significant losses on any crop. Taking advantage of the fact that this species produces prolific numbers of perithecia in culture, the genome of *F. neocosmosporiellum* was sequenced and transcriptomic analysis across five stages of perithecium development was performed to better understand the metabolic potential for sexual development and gain insight into its life history. Perithecium morphology together with the genome and transcriptome were compared with those of the plant pathogen *F. graminearum*, a model for studying perithecium development. Larger ascospores of *F. neocosmosporiellum* and their tendency to discharge as a cluster demonstrated a duality of dispersal: the majority are passively dispersed through the formation of cirrhi, while a minority of spores are shot longer distances than those of *F. graminearum*. The predicted gene number in the *F. neocosmosporiellum* genome was similar to that in *F. graminearum*, but *F. neocosmosporiellum* had more carbohydrate metabolism-related and transmembrane transport genes. Many transporter genes were differentially expressed during perithecium development in *F. neocosmosporiellum*, which may account for its larger perithecia. Comparative analysis of the secondary metabolite gene clusters identified several polyketide synthase genes that were induced during later stages of perithecium development. Deletion of a polyketide synthase gene in *F. neocosmosporiellum* resulted in a defective perithecium phenotype, suggesting

an important role of the corresponding metabolite, which has yet to be identified, in perithecium development. Results of this study have provided novel insights into the genomic underpinning of development in *F. neocosmosporiellum*, which may help elucidate its ability to occupy diverse ecological niches.

Keywords: perithecium, *Fusarium*, transcriptome, mating type locus, secondary metabolic genes, sexual development

INTRODUCTION

Flask-shaped fruiting bodies called perithecia predominate in the class Sordariomycetes within the Ascomycota of the Kingdom Fungi. This class contains some of the most problematic plant and insect pathogens, and saprotrophs, including the genetic model *Neurospora crassa*. Evolution has bequeathed evolvable features to the perithecia of Sordariomycetes, conveying the ability to disperse spores most efficiently according to niche (Trail, 2007). The genomics of perithecium production has been most extensively studied in *Fusarium graminearum* and *N. crassa*. *F. graminearum* is an important pathogen of grain crops and perithecia contribute significantly to its disease cycle (Desjardins et al., 2006). Genes involved in perithecium development have been identified through transcriptomics and genomics studies, leading to large-scale gene function analyses (Son et al., 2011; Wang et al., 2012; Trail and Gardiner, 2014). Most recently, a study of the ancestral levels of transcription in *Fusarium* and *Neurospora* species have revealed genes that play significant roles in their divergent morphologies (Trail et al., 2017).

Ascospores are the products of meiosis and are formed within perithecia in the majority of Sordariomycetes. Typically eight ascospores are formed within an ascus, which when fully developed provides sufficient turgor pressure to forcibly discharge ascospores into the air above perithecia, thereby dispersing them. Ascospores vary in size, shape, ornamentation, and pigmentation. These features can affect dispersal distance, survival in air due to UV damage, and other factors (Trail, 2007). Species are homothallic (self-fertile) or heterothallic (self-sterile), and mating type is determined by the presence of *MAT1-1* and/or *MAT1-2* idiomorphs. Idiomorph is the term used to describe the two forms of the mating type locus in the Ascomycota. Within a species, *MAT1-1* and *MAT2-1* idiomorphs occur at the same genomic location, but they are not considered alleles, because genes in the two idiomorph types are not homologous (Metzenberg and Glass, 1990). Thus, in heterothallic *Fusarium* species, the *MAT1-1* idiomorph includes the *MAT1-1-1*, *MAT1-1-2*, and *MAT1-1-3* genes, while the *MAT1-2* idiomorph includes the *MAT1-2-1* and *MAT1-2-3* genes. In the homothallic species *F. graminearum*, by contrast, the *MAT* locus includes all five of these genes.

Fusarium species occupy a wide variety of niches, and include many important plant pathogens and a number of opportunistic human pathogens (O'Donnell et al., 2010), soil saprotrophs, insect parasites, and plant endophytes (Rodriguez et al., 2009). *Fusaria* are notorious for producing toxic secondary metabolites

(mycotoxins) that can contaminate food and feed, rendering it unsafe for consumption by humans and other animals. Synthesis of these and other secondary metabolites typically involves non-ribosomal peptide synthase (NRPS), polyketide synthase (PKS), prenyltransferase, and/or terpene synthase enzymes that catalyze synthesis of structures that typically undergo one or more subsequent modifications. In fungi, genes encoding these enzymes are often found clustered with genes encoding modifying enzymes such as acetyltransferases, methyltransferases, dehydrogenases, and monooxygenases that are required for biosynthesis of the final products. Production of secondary metabolites is often associated with niche-specific adaptations (Turgeon and Bushley, 2010).

The *Fusarium sambucinum* (FSAMSC) and *F. solani* (FSSC) species complexes are among the most agriculturally important and species-rich lineages within the genus (O'Donnell et al., 2013). In prior research, we studied the homothallic, cereal pathogen *F. graminearum* (FSAMSC) with particular emphasis on development and function of perithecia, as well as production of mycotoxins and other secondary metabolites (Gaffoor et al., 2005; Sikhakolli et al., 2012; Wang et al., 2012, 2018; Trail et al., 2017; Kim et al., 2018). Recently, we began a study of perithecium development in homothallic *F. neocosmosporiellum* (formerly *Neocosmospora vasinfecta*; Geiser et al., 2013), a member of the FSSC that is reported to be pathogenic on peanut and soybean (Dau et al., 2010; Pan et al., 2010; Sun et al., 2014; Greer et al., 2015), and an opportunistic pathogen of humans (Cornely et al., 2001; Gabriel et al., 2013). This cosmopolitan species has also been reported on infected soybean cyst nematodes (Gintis et al., 1983) and dung of diverse herbivores (Calaça et al., 2013). It also possesses a highly active CO₂ fixation mechanism (Budd, 1969). To better understand the metabolic potential of this fungus, we sequenced the genome of *F. neocosmosporiellum* NRRL 22166 and compared its gene content with previously published *F. graminearum* genomes. Both are homothallic and prolific producers of perithecia, but their niches, and perithecium and ascospore morphology are quite divergent. We performed transcriptomics across stages of perithecium development to better understand differences in morphology and function of the perithecia in these species.

MATERIALS AND METHODS

Fungal Strain and Genome Sequencing

Fusarium neocosmosporiellum NRRL 22166 was isolated from the soybean cyst nematode *Heterodera glycines* in southern

Illinois in 1983 (O'Donnell, 2000). To prepare DNA for genome sequencing, *F. neocosmosporiellum* was grown in YEPD medium (0.1% yeast extract, 0.1% peptone, 2% glucose) for 2 days at room temperature on a rotary shaker set at 200 rpm. Mycelia were harvested by filtration, lyophilized, ground to a powder, and genomic DNA was extracted using the ZR Fungal/Bacterial DNA MiniPrep kit (Zymo Research, Irvine, CA, United States). A DNA library was prepared from genomic DNA with the Nextera XT DNA library Preparation Kit using the protocol specified by the manufacturer (Illumina, Inc., San Diego, CA, United States). Sequence reads were generated from the library using a paired-end approach with a MiSeq Illumina platform (Illumina, Inc.). Reads were processed and assembled using CLC Genomics Workbench (Qiagen Inc.) (Supplementary Table S1). Completeness of the assembled genome was evaluated by BUSCO (v1.22) using 'Sordariomyceta odb9' database (Simão et al., 2015).

Sexual Stage Induction and RNA-seq

Fusarium neocosmosporiellum was maintained on potato dextrose agar (PDA) plates, then grown in carboxymethylcellulose medium for 4 days to produce microconidia (Cappellini and Peterson, 1965). Carrot agar plates (60 mm in diameter) (Klittich and Leslie, 1988) were inoculated by spreading 50 μ l of a 10^5 spores/ml conidial suspension across the surface of the agar, which was incubated at room temperature under constant light. Two days after incubation, aerial hyphae and conidia were removed by gently scraping the culture surface with a spatula, and then 0.9 ml of 2.5% Tween 60 (Sigma-Aldrich, St. Louis, MO, United States) was applied to the surface to induce perithecia. Hyphae and perithecial tissues were collected when the six successive developmental stages delineated by Sikhakolli et al. (2012) were observed. The stages are as follows: S0–2 h after the Tween 60 application, which represents the immediate reaction to possible physical damage of hyphae and Tween 60, but does not reflect significant development; S1–formation of ascogonia (fertile hyphae that function as the 'female' during the sexual cycle, which are subsequently enveloped by perithecial tissues); S2–formation of perithecial walls; S3–formation of paraphyses (sterile hyphae interspersed with asci in a perithecium); S4–formation of asci (sac-like structures in which meiosis occurs followed by a synchronous round of mitosis); S5–formation of eight uniseriate ascospores.

Total RNA was extracted from hyphae and perithecial tissues ground in liquid nitrogen using TRIzol reagent (Thermo Fisher Scientific, Waltham, MA, United States) according to the manufacturer's instructions together with the following extraction steps: two phenol (pH 4.6)-chloroform-isoamyl alcohol (25:24:1) extraction steps followed by two chloroform extraction steps after the initial TRIzol-chloroform phase separation. RNA pellets were dissolved in 88 μ L of nuclease-free water and subjected to genomic DNA digestion with DNase (Qiagen Inc.). RNA samples were then concentrated using RNA Clean & Concentrator (Zymo Research). RNA quality was confirmed using an Agilent 2100 Bioanalyzer

(Agilent Technologies, Palo Alto, CA, United States). Two micrograms of total RNA per sample was used for cDNA library construction. Strand-specific cDNA libraries were constructed from poly-A captured RNAs using the KAPA Stranded RNA-Seq Library Preparation Kit (Kapa Biosystems, Wilmington, MA, United States) and sequenced on an Illumina HiSeq 2500 platform (Illumina Inc.; single-end 50 bp reads) at Michigan State University's Research Technology Support Facility¹.

Ascospore Release

Forcible spore discharge was studied as previously described (Trail et al., 2005). In brief, the horizontal distance that spores traveled was measured in a glass chamber to minimize free convection current (Aylor and Anagnostakis, 1991). Perithecium formation was induced on carrot agar so that the spores were ejected lengthwise down the coverslip, which covered the length of the 6 cm chamber. The discharged spores were examined by removing the coverslip on which the agar rested and the cover slip in the line of fire at the end of the chamber.

RNA-seq Data Processing and Genome Annotation

The quality of raw reads was assessed with FastQC (v0.11.3)². Poor quality reads were trimmed or filtered out, and adapters and homopolymers were trimmed from raw reads using ngsShoRT (v2.2; Chen et al., 2014) with option arguments: '-lqs 12', '-tera_avg 20', '-5a_mp 98', and '-rmHP_ml 10.' Filtered reads were mapped to the *F. neocosmosporiellum* genome using HISAT2 (v2.0.4; Kim D. et al., 2015). Functional annotation of the genome was performed using MAKER2 (Holt and Yandell, 2011). RNA-seq data for the six developmental stages was provided as transcript evidence to improve gene models prediction by MAKER2, yielding a total of 14,353 gene models. Ensembl annotation version 32 of the *F. graminearum* PH-1 genome was used, (accessions: FGSC9075/NRRL 31084) (King et al., 2015) as well as the transcriptome data during perithecium development (Kim et al., 2018). Orthologous genes shared by the two fungi

¹<https://rtsf.natsci.msu.edu/genomics>

²www.bioinformatics.babraham.ac.uk/projects/fastqc

TABLE 1 | Genome summary and completeness.

| | <i>F. graminearum</i> ^a | <i>F. neocosmosporiellum</i> |
|----------------------------------|------------------------------------|------------------------------|
| Genome size (bp) | 36,563,796 | 54,657,069 |
| GC (%) | 48.0 | 51.4 |
| Predicted genes (#) | 14,164 | 14,353 |
| Expressed genes (#) ^b | 12,024 | 12,486 |
| BUSCO complete (%) | 96 | 93 |
| BUSCO fragmented (%) | 3 | 5 |
| BUSCO missing (%) | 1 | 2 |

^aBased on genome assembly version RRes v4.0 (King et al., 2015). ^bFiltered by an expression threshold (see Materials and Methods).

were grouped by OrthoMCL using an inflation value of 2.5 (Li et al., 2003).

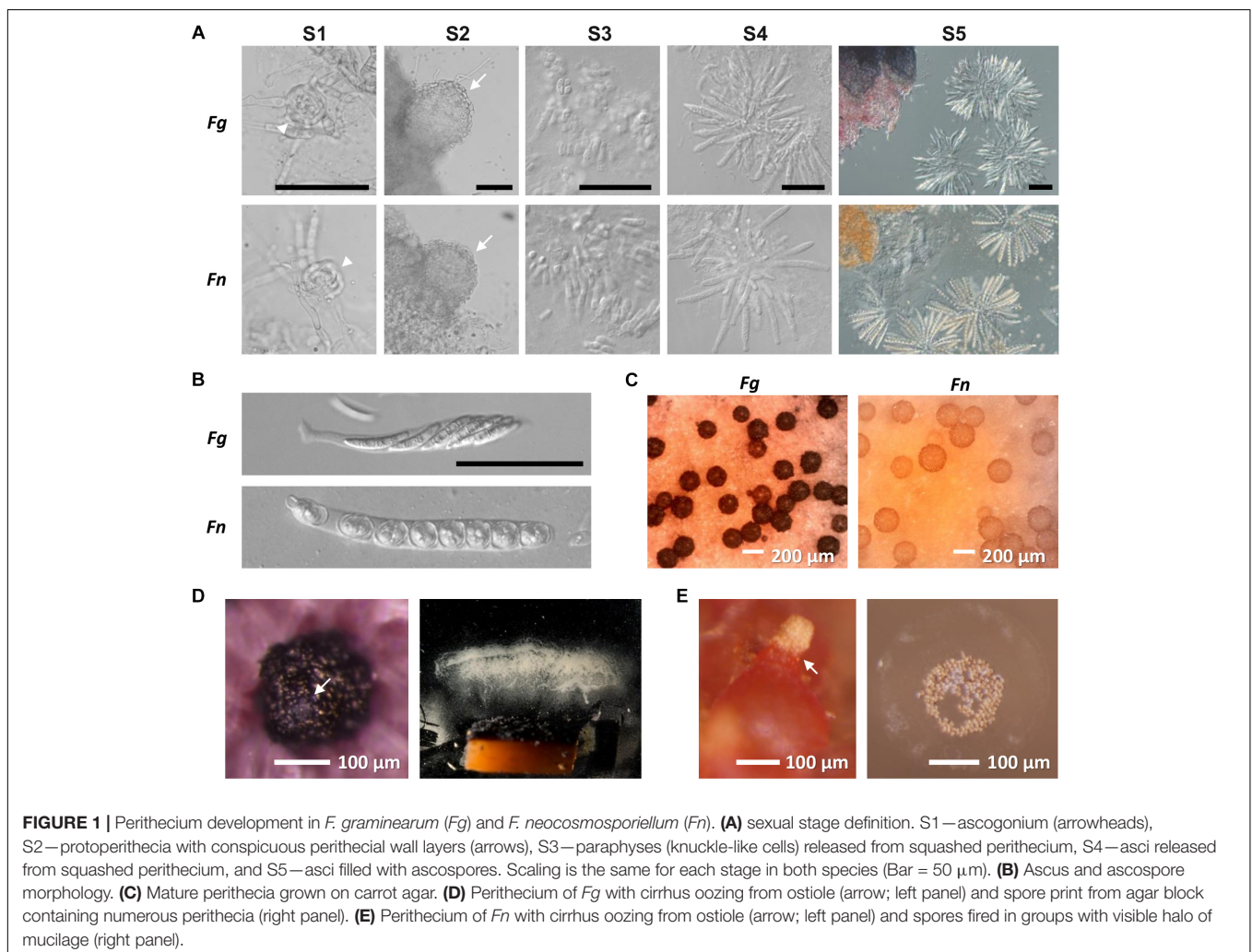
Identification of CAZyme Genes and Secondary Metabolite Biosynthetic Gene Clusters

Carbohydrate-active enzyme (CAZyme) families involved in the breakdown, biosynthesis, or modification of carbohydrates and glycoconjugates (Lombard et al., 2014) were detected by running *hmmscan* in HMMER (v3.1b2; Eddy, 2011), with an *E*-value cutoff of 1×10^{-10} . Hidden Markov model (HMM) profiles for CAZyme families were acquired from the dbCAN v6.0 database (Huang et al., 2018). When overlapping modules were detected, the one with the lowest *E*-value was retained. Genes annotated as one of the four CAZyme families (GH, GT, PL, and CE) were included, and the predicted CAZyme genes with a covered fraction of HMMs lower than 0.30 were excluded. Secondary metabolite biosynthetic gene clusters were predicted using antiSMASH (v4.0.2; Medema et al., 2011) with a default setting (accessed November 2, 2017). Of the 35 biosynthetic gene clusters identified in the

F. neocosmosporiellum genome, we analyzed the type I-PKS, NRPS, and terpene gene clusters.

Differential Expression and Functional Enrichment Analyses

Read counts for the annotated genes were calculated using *htseq-count* (v0.6.1; Anders et al., 2015) in *F. graminearum* and *F. neocosmosporiellum*. Gene expression levels in counts-per-million (CPM) values were computed and normalized by effective library size estimated by ‘trimmed mean of *M*-values’ using edgeR (v3.14.0; Robinson et al., 2010). We defined expressed genes when a gene had CPM values greater than 1 in at least 3 samples. Expressed genes with $\log_2[\text{fold-change}]$ greater than 1.5 between two successive developmental stages were identified as differentially expressed (DE) at a 5% false discovery rate (FDR) using limma (v3.28.21; Law et al., 2016). Gene ontology (GO) terms were assigned to the genomes of the two fungi using Trinotate (v3.0.1; Bryant et al., 2017). The list of GO terms was customized by adding several GO terms related to developmental processes to the GO Slim terms specific for fission yeast as described in



Kim et al. (2018). Functional enrichment analyses for DE genes were performed using Goseq (v1.24.0), including only those genes annotated by one or more GO terms (Young et al., 2010). To assess enrichment of GO terms, the Wallenius approximation, which is an extension of the hypergeometric distribution, and the Benjamini-Hochberg method were used to calculate the FDR-corrected (adjusted) *P*-value.

Coexpression Network Analysis

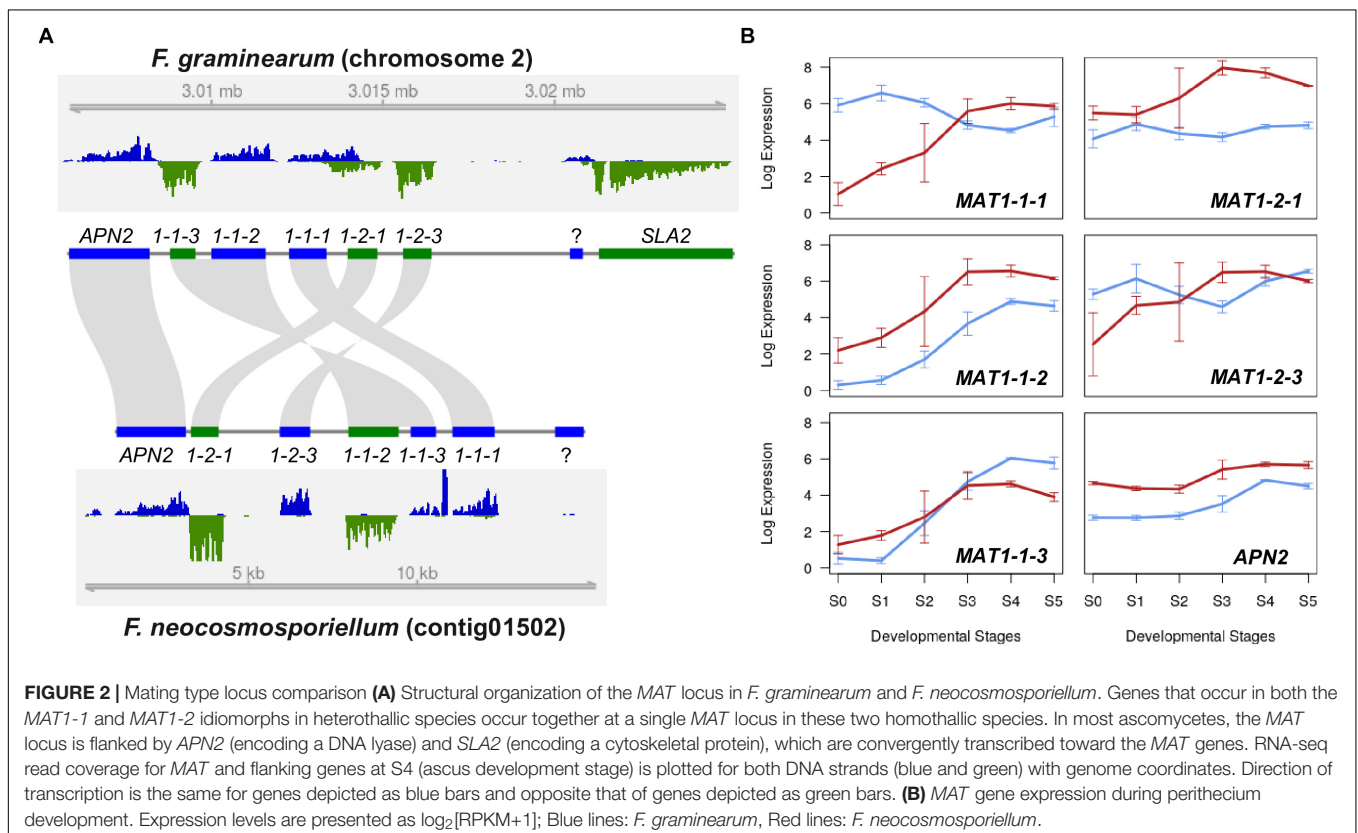
The weighted gene correlation network analysis (WGCNA) R package (v1.51; Langfelder and Horvath, 2008) was used to cluster CAZyme genes by averaged RPKM values across developmental stages. The 'pickSoftThreshold' function was used to determine soft-thresholding power that measures the strength of correlation based on the direct correlation value of pairs of genes and the weighted correlations of all of their shared neighbors in the network space. The soft-thresholding power 28 and 15 were selected, respectively, for *F. graminearum* and *F. neocosmosporiellum* CAZyme genes. A range of treecut values was tested for cluster detection, and the value was set to 0.18, which corresponding to a correlation of 0.82. All other WGCNA parameters were set at the default.

Generation of Targeted Gene-Deletion Mutants

To generate gene replacement mutants, we used double-joint PCR and split-marker strategies with a minor modification

(Catlett et al., 2003; Yu et al., 2004). For the first round of PCR, upstream (left flanking) regions and downstream (right flanking) regions of the coding sequence of target genes (*PKS7*, *PKS35* and *TC2*) were amplified using L5 and L3 primer pairs and R5 and R3 primer pairs, respectively. L3 and R5 primers have 27 nt-long overhang sequences complementary to the 5' and 3' ends of a 1,376-bp hygromycin phosphotransferase gene (*hph*) cassette that was amplified from the pCB1004 plasmid (Carroll et al., 1994) using the HYG5 and HYG3 primers. In the second round of PCR, left and right flanking regions were fused to the *hph* cassette through PCR by overlap extension. For amplification of split marker constructs, one microliter of the PCR product from the second round was used as template for the third round of PCR with the following nested primer pairs: N5 and HY-R pairs to generate 5'-split constructs, and YG-F and N3 pairs to generate 3'-split constructs. The split marker constructs were introduced into protoplasts by polyethylene glycol-mediated genetic transformation as described in Hallen-Adams et al. (2011). Target gene replacement with the *hph* cassette was verified in transformants by diagnostic PCRs (Supplementary Figure S1).

Genetic complementation of the Δ *PKS7* strain was accomplished by introducing the *PKS7* locus, which includes the *PKS7* coding sequence plus 700 and 300 bp of the upstream and downstream sequences, respectively. The 5' half (3,498 bp) and 3' half (6,287 bp) of the *PKS7* gene locus were amplified separately using primer sets *PKS7*-5H and *PKS7*-3H, respectively. Then, the two PCR fragments and the pDS23 plasmid (Teichert et al., 2012),



which were pre-cut with *AvrII* and *BglIII*, were assembled using a Gibson Assembly reagent (New England Biolabs Inc., Ipswich, MA, United States). Importantly, the two fragments of the *PKS7* gene were designed to be assembled at an intron region to avoid a possible frameshift due to misassembly. Reintroduction of the *PKS7* gene locus was confirmed by PCR (**Supplementary Figure S1**). Primers used in targeted gene knockouts and genetic complementation are listed in **Supplementary Table S2**.

Data Accession

The *F. neocosmosporiellum* NRRL 22166 genome sequence can be accessed through accession number SSHR0000000 in NCBI. The RNA-seq data generated in the present study was deposited in NCBI's Gene Expression Omnibus and is accessible through GEO series accession number GSE124553.

RESULTS

Perithecium Development, Genome, and Transcriptomes of *F. neocosmosporiellum*

De novo sequence assembly of MiSeq-generated reads of *F. neocosmosporiellum* resulted in 50× coverage and an estimated genome size of 54,657,069 bp. The GC content of the *F. neocosmosporiellum* genome (51.4%) was slightly higher than that of *F. graminearum* (48.3%), but it is comparable to a closely-related species reported as *F. solani* f. sp. *pisi* (51.7%) (Coleman et al., 2009). Similar to other *Fusarium* species (King et al., 2018), a total of 14,353 genes were predicted using the MAKER2 gene modeling program (Holt and Yandell, 2011). Completeness of the sequenced genome was quantified by the presence of core eukaryotic genes and was shown to be comparable to that of the finished *F. graminearum* genome and other related species (**Table 1** and **Supplementary Figure S2**). To compare the transcriptional profile of *F. neocosmosporiellum* to that of *F. graminearum* during perithecium development, *F. neocosmosporiellum* RNA samples from vegetative hyphae after sexual induction (S0) and from five successive sexual stages (S1–S5) were sequenced and used in the comparative studies (**Figure 1A**). Mature perithecia of both species containing asci with ascospores are compared in **Figures 1B,C**. A total of 680 million RNA-seq reads were generated from 18 samples (6 stages × 3 replicates), with an average of 37 million mapped reads per sample (**Supplementary Figure S3**).

Ascospore Dispersal

Spore dispersal from mature perithecia took two forms. Spores forcibly discharged were primarily deposited on the far end of the chamber, with a few ascospores landing at the coverslip base and a few on the ceiling of the chamber. Compared to the quantity of discharged ascospores from *F. graminearum* (**Figure 1D**; Trail et al., 2005), the ascospore numbers that accumulated on the coverslip supporting perithecia were exceedingly low, amounting to less than 8 ascospores per perithecium. The vast majority of perithecia eventually exuded ascospores *en masse*

in the form of cirrhi (**Figure 1E**). In addition, ascospores on the cover slip at the far end of the chamber indicated that spores landed in groups, suggesting that they likely remained together when ejected and during flight. A mucilaginous halo was visible surrounding groups of ascospores (**Figure 1E**). Attempts to dislodge the ascospores by adding a drop of water and leaving it up to 3 h were unsuccessful for the majority of the spores, as less than 10% dislodged.

TABLE 2 | Annotation of expressed CAZyme in *Fusarium graminearum* (*Fg*) and *F. neocosmosporiellum* (*Fn*).

| Classification ^a | CAZyme families (enzyme activity) | <i>Fg</i> | <i>Fn</i> |
|---|--|------------------------|------------------------|
| CAZymes (expressed) ^b | CE: Carbohydrate esterases | 93 | 88 |
| | GH: Glycoside hydrolases | 224 | 211 |
| | GT: Glycosyl transferases | 81 | 91 |
| | PL: Polysaccharide lyases | 18 | 23 |
| | Total | 416 (481) ^c | 413 (551) ^c |
| Cellulose | GH1 (β -glucosidase, etc.) | 3 | 3 |
| | GH5 (cellulase, etc.) | 1 | 3 |
| | GH6 (endoglucanase and cellobiohydrolase) | 1 | 0 |
| | GH45 (endoglucanase) | 1 | 1 |
| | GH74 (reducing end cellobiohydrolase) | 1 | 1 |
| | Subtotal | 7 | 8 |
| | Subtotal | 7 | 8 |
| Pectin | CE8 (pectin methyltransferase) | 3 | 3 |
| | CE12 (pectin acetyltransferase) | 3 | 1 |
| | GH105 (rhamnogalacturonyl hydrolase, etc.) | 3 | 2 |
| | PL1 (pectate lyase, etc.) | 8 | 9 |
| | PL3 (pectate lyase) | 6 | 7 |
| | PL9 (hyaluronate lyase, etc.) | 0 | 1 |
| | Subtotal | 23 | 23 |
| Xylan and hemicellulose sidechain modifications | CE1 (acetyl xylan esterase, etc.) | 6 | 7 |
| | CE2 (acetyl xylan esterase) | 1 | 0 |
| | CE3 (acetyl xylan esterase) | 5 | 5 |
| | CE4 (acetyl xylan esterase, etc.) | 6 | 6 |
| | CE5 (acetyl xylan esterase and cutinase) | 9 | 3 |
| | GH10 (endo- β -1,4-xylanase, etc.) | 1 | 1 |
| | GH11 (endo- β -1,3-xylanase, etc.) | 2 | 1 |
| | GH43 (β -xylosidase, etc.) | 12 | 12 |
| | GH57 (α -amylase, etc.) | 1 | 1 |
| | GH62 (α -L-arabinofuranosidase) | 1 | 0 |
| | GH67 (α -glucuronidase, etc.) | 1 | 0 |
| | GH95 (α -L-fucosidase, etc.) | 2 | 1 |
| | GH115 (xylan α -1,2-glucuronidase etc.) | 2 | 1 |
| | Subtotal | 49 | 38 |

^aCAZyme classification by targeting plant cell wall carbohydrate, as in Gruninger et al. (2018). ^bFiltered by an expression threshold (see Materials and Methods). ^cTotal predicted CAZyme genes in parentheses (E -value < 10^{-10}).

MAT Locus in *F. neocosmosporiellum*

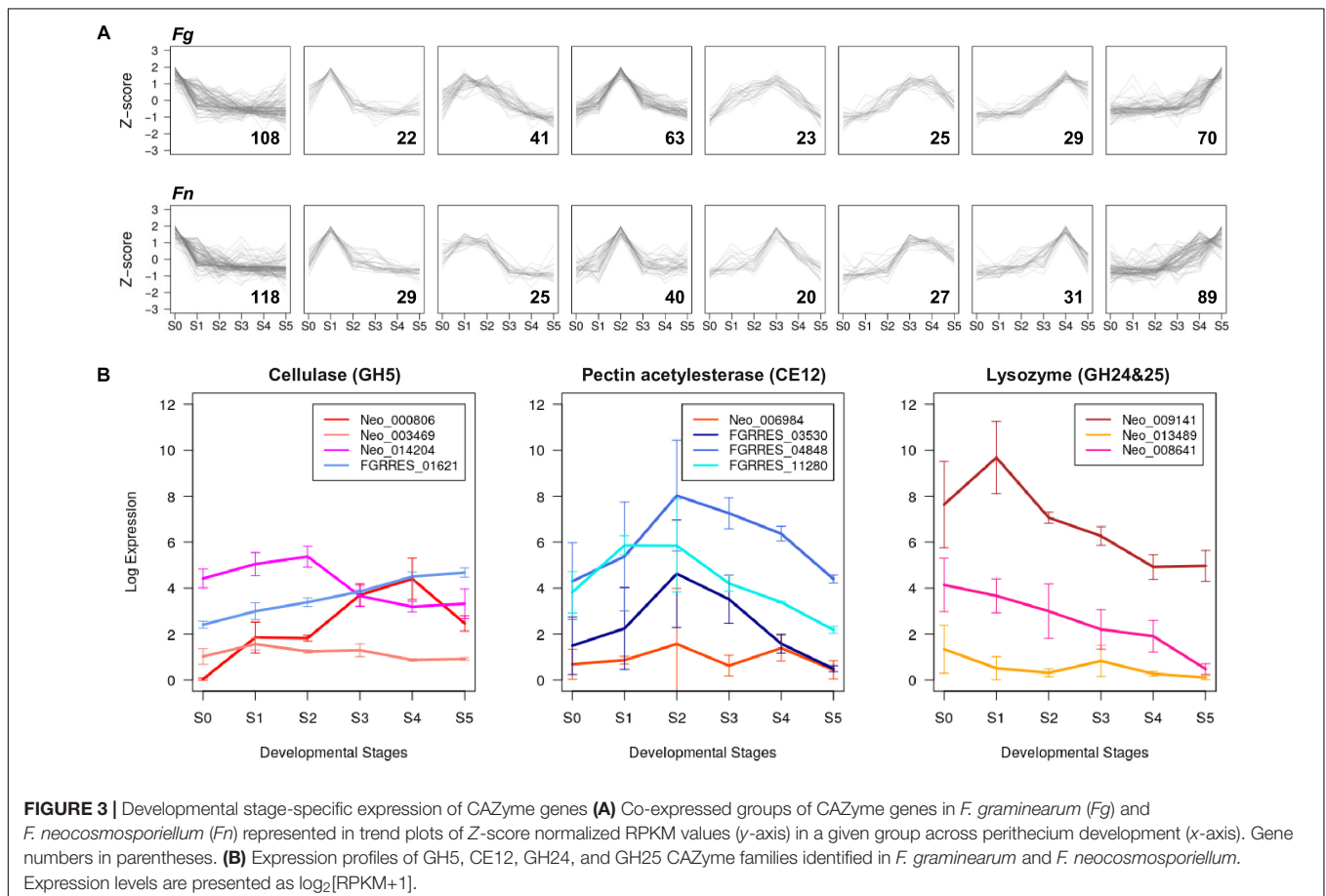
Fusarium neocosmosporiellum is homothallic (self-fertile), and sequence analysis indicated that its mating type locus includes both *MAT1-1* and *MAT1-2* genes. Although the *MAT* locus in *F. neocosmosporiellum* and *F. graminearum* include both *MAT1-1* and *MAT1-2* genes, the order of the *MAT* genes and their direction of transcription differs in these two homothallic species (Figure 2A). Organization of the *MAT* genes suggests that they have been rearranged by one or two inversions relative to closely related species in the FSSC. One inversion involved *MAT1-1-3* and *MAT1-1-2*, the order of which is inverted compared to closely related fusaria (Hughes et al., 2014), and the other inversion involved *MAT1-2-3*, which was divergently transcribed from *MAT1-2-1* in *F. neocosmosporiellum*, but not in closely related fusaria (Hughes et al., 2014). However, the ancestral state of the transcriptional direction of *MAT1-2* genes in the FSSC remains to be determined (Hughes et al., 2014).

In addition to differences in gene organization, expression of *MAT* genes during perithecium development differed in the two fungi. In *F. neocosmosporiellum*, expression of all five *MAT* genes appeared to be synchronized and gradually increased throughout perithecium development (Figure 2B). By contrast, the *MAT1-1-1*, *MAT1-2-1*, and *MAT1-2-3* in *F. graminearum* were already expressed at earlier stages, slightly

decreased, then increased again at later stages (Figure 2B), which is consistent with the previous expression studies, and real-time PCR data (Kim et al., 2012). Interestingly, our strand-specific RNA-seq data revealed that the *MAT1-1-1* and *MAT1-2-1* genes in *F. graminearum* possessed an extended 3' untranslated region, and the convergently transcribed genes overlapped each other, while no such overlap was observed in *F. neocosmosporiellum* (Figure 2A).

CAZyme Gene Expression During Perithecium Development

The annotated *F. neocosmosporiellum* genome was predicted to contain more genes classified as CAZymes (i.e., genes involved in the breakdown and modification of polysaccharides; Lombard et al., 2014), compared to *F. graminearum* (E -value $< 10^{-10}$; Table 2). However, the perithecium transcriptome data indicated that the number of CAZyme genes expressed during perithecium development was similar in the two species (Table 2). Co-expression analyses showed that many of the expressed CAZyme genes were induced in different developmental stages in the two fusaria, suggesting they play unique roles during perithecium development (Figure 3A). The CAZyme genes in the two species comprised about 3.4% of the gene content. Although the percentage of CAZyme genes was similar in both, some differences between the species were observed.

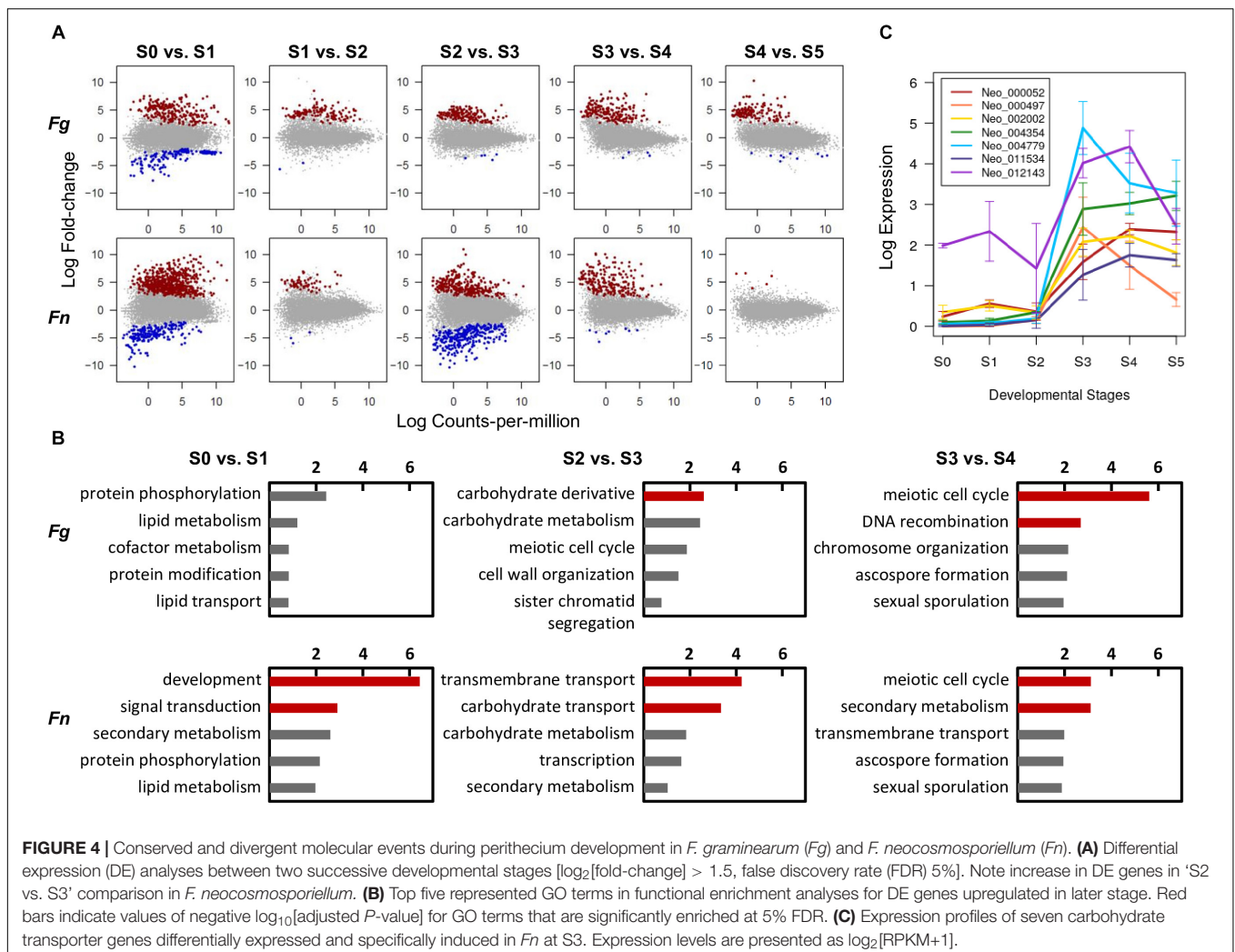


Fusarium neocosmosporiellum possesses three genes in the CAZyme family GH5, which targets cellulose, while *F. graminearum* contained only one gene in this family (Table 2). Although one of the three GH5-family genes, Neo_003469, exhibited low expression levels throughout perithecium development, the other two genes, Neo_014204 and Neo_000806, were induced at early and late stages, respectively, of perithecium development (Figure 3B). Expression of the sole GH5-family gene in *F. graminearum* was relatively constitutive. *Fusarium graminearum* possesses three genes in the CAZyme family CE12, which targets pectin, while *F. neocosmosporiellum* contained only one gene in this family (Table 2). The CE12-family genes, FGRRES_03530, FGRRES_04848 and FGRRES_11280, in *F. graminearum* were highly induced at earlier developmental stages than the single CE12-family gene, Neo_006984, in *F. neocosmosporiellum* (Figure 3B). Also, *F. neocosmosporiellum* possesses three genes in the CAZyme families GH24 and GH25, which putatively target bacterial cell walls (i.e., peptidoglycan) (Zhao et al., 2013). These genes were expressed during earlier developmental stages, followed by gradual decline in expression during later stages

(Figure 3B). The GH24- and GH25-family genes were absent in *F. graminearum*.

Transcriptome Changes During Perithecium Development

To search for genes that play important roles in *F. neocosmosporiellum* and *F. graminearum*, we identified DE genes unique to each developmental stage. Overall, upregulated genes were predominant in advanced developmental stages in the differential expression analyses, suggesting that gene induction mechanisms represent a common means for gene regulation during perithecium development (Figure 4A). In *F. neocosmosporiellum*, perithecial volume dramatically increased within a relatively short period time between S2 and S3 (48 h). This process resulted in much larger perithecia when compared to *F. graminearum* (Figure 1C), which required 24 h for the same developmental interval. Accordingly, numerous DE genes were identified between S2 and S3 in *F. neocosmosporiellum*, indicating that many cellular processes were active (Figure 4A).



To identify the main cellular events that took place at each stage of perithecium development, we performed functional enrichment analyses for DE genes upregulated in advanced stages. As a result, genes from similar families were found to be enriched in both fusaria. For example, meiosis-related genes were commonly enriched for the GO term ‘meiotic cell cycle process’ at 5% FDR in both species when perithecia reached maturity and asci developed (Figure 4B). Nevertheless, we observed a striking difference in the ‘S2 vs. S3’ comparison, in which nutrient transport-related genes were significantly enriched for GO terms ‘transmembrane transport’ and ‘carbohydrate transport’ in *F. neocosmosporiellum*. The GO term ‘transmembrane transport’ had 30 child (direct descendent) GO terms with more specific annotations related to transport of various cellular substrates. Among them, we examined 15 GO terms relevant to fungi and found that *F. neocosmosporiellum* possessed approximately 50% more genes related to carbohydrate transmembrane transport (GO:0034219) in *F. graminearum* (67 vs. 44; Table 3). Orthologous gene cluster analyses showed that there were

26 carbohydrate transmembrane transport genes present in *F. neocosmosporiellum*, whereas most of the *F. graminearum* genes (40 out of 44) grouped with *F. neocosmosporiellum* orthologs. Among the 67 carbohydrate transporter genes in *F. neocosmosporiellum*, seven were DE and specifically induced at S3 (Figure 4C).

Secondary Metabolite Biosynthetic Genes

Functional enrichment analyses indicated that many secondary metabolism-related genes were upregulated during perithecium development in *F. neocosmosporiellum*, especially during later stages (S3 vs. S4; Figure 4B). Using antiSMASH, we identified a total of eleven PKSs, nine NRPSs, and three terpene biosynthesis-related genes (TCs) in the *F. neocosmosporiellum* genome. Among these, a total of eight PKSs, four NRPSs, and three TCs genes were expressed in our transcriptome datasets (Table 4). Orthologs of all of the expressed secondary metabolite-related genes, except an NRPS gene (*SimA*), occur in the closely related species *F. euwallaceae* and *F. solani* f. sp. *pisi*, which are members of the FSSC. The proteins encoded by these genes shared amino acid (AA) sequence similarities ranging from 80 to 98% (Table 4). An NRPS gene homologous to *SimA* was predicted to encode a 15,274 AA-long polypeptide, showing 96% sequence similarity with the cyclosporine synthetase *SimA* in *Tolypocladium inflatum* (Bushley et al., 2013).

Some PKS and NRPS genes in *F. neocosmosporiellum* and *F. graminearum* were orthologous, while others were not (Table 4). In *F. graminearum*, *PKS3* (also known as *PGL1* and *FSR1*) has been shown to be involved in synthesis of the black pigment in the perithecial walls (Gaffoor et al., 2005; Frandsen et al., 2016). However, sexually reproducing species in the FSSC, including *F. neocosmosporiellum*, produce orange to red perithecia. *PKSN* was reported to be responsible for the red pigment in the perithecial walls in another phylopecies within the FSSC (Graziani et al., 2004). AntiSMASH identified a *PKSN* homolog in *F. neocosmosporiellum* (henceforth *PKS35*; Brown and Proctor, 2016) and predicted the *PKS35* gene cluster. The boundaries of this putative cluster were further supported by the co-expression of genes within it (Figure 5A). We identified ten co-regulated genes, including the *PKS35*, whose expression peaked at ‘S3’ when pigmented perithecial walls form (Figure 5A). Interestingly, five of the genes in the putative *PKS35* gene cluster are homologs of the five genes in the gene cluster responsible for biosynthesis of herqueinone, a red pigment produced by *Penicillium herquei* (Stodola et al., 1951; Gao et al., 2016) (Figure 5A).

In *F. neocosmosporiellum*, secondary metabolite biosynthetic (SM) genes that were expressed in our transcriptome data could be categorized by their expression patterns: (1) constitutive expression during all stages of perithecium development, (2) reduced after sexual induction, (3) induced at earlier stages (S1–S2), and (4) induced at later stages (S3–S5) (Figure 5B). Several SM genes, including the *SimA*, exhibited constitutive expression at all stages of perithecium

TABLE 3 | Transporter genes expressed during perithecium development in *Fusarium graminearum* (*Fg*) and *F. neocosmosporiellum* (*Fn*).

| Gene ontology ID number and description | <i>Fg</i> | <i>Fn</i> |
|---|-------------------------------------|------------|
| GO:0055085 transmembrane transport | 772 ^a (839) ^b | 917 (1196) |
| GO:0034219 carbohydrate transmembrane transport | 44 (50) | 67 (87) |
| GO:1901264 carbohydrate derivative transport | 83 (91) | 95 (128) |
| GO:0071806 protein transmembrane transport | 44 (44) | 48 (51) |
| GO:1901679 nucleotide transmembrane transport | 55 (61) | 61 (85) |
| GO:0015780 nucleotide-sugar transmembrane transport | 5 (5) | 5 (5) |
| GO:0006855 drug transmembrane transport | 28 (28) | 34 (39) |
| GO:0035382 sterol transmembrane transport | 1 (1) | 1 (1) |
| GO:0035461 vitamin transmembrane transport | 8 (10) | 7 (17) |
| GO:1903825 organic acid transmembrane transport | 129 (142) | 157 (216) |
| GO:0044718 siderophore transmembrane transport | 2 (2) | 3 (3) |
| GO:0034220 ion transmembrane transport | 314 (336) | 368 (454) |
| GO:0034486 vacuolar transmembrane transport | 15 (15) | 15 (17) |
| GO:1990542 mitochondrial transmembrane transport | 47 (47) | 49 (51) |
| GO:0098739 import across plasma membrane | 18 (22) | 23 (28) |
| GO:0034762 regulation of transmembrane transport | 48 (52) | 49 (55) |

^aFiltered by an expression threshold (see Materials and Methods). ^bTotal predicted genes in parentheses (E -value < 10^{-5}).

TABLE 4 | Secondary metabolite biosynthetic genes.

| <i>F. neocosmosporiellum</i> ^a | Best hit in <i>F. graminearum</i> ^a | % ^b | Best hit in NCBI database ^c | % ^b |
|---|--|----------------|---|----------------|
| PKS2 (Neo_003331) | PKS2 (FGRRES_04694) | 55 | <i>F. euwallaceae</i> (ALQ32835) | 82 |
| PKS3 (Neo_007042) | PKS3 (FGRRES_17168) | 76 | <i>F. euwallaceae</i> (ALQ32837) | 95 |
| PKS7 (Neo_006055) | PKS7 (FGRRES_08795) | 62 | <i>F. euwallaceae</i> (ALQ32840) | 80 |
| PKS22 (Neo_009895) | PKS11 (FGRRES_01790) | 42 | <i>F. euwallaceae</i> (ALQ32841) | 93 |
| PKS30 (Neo_001289) | PKS5 (FGRRES_17677) | 36 | <i>F. euwallaceae</i> (ALQ32842) | 90 |
| PKS31 (Neo_001313) | PKS11 (FGRRES_01790) | 41 | <i>F. solani</i> f.sp. <i>pisi</i> (XP_003041774) | 87 |
| PKS33 (Neo_000291) | PKS11 (FGRRES_01790) | 52 | <i>F. euwallaceae</i> (ALQ32839) | 95 |
| PKS35 (Neo_002749) | PKS12 (FGRRES_02324) | 44 | <i>F. solani</i> f.sp. <i>pisi</i> (AAS48892) | 93 |
| NRPS2 (Neo_002267) | NRPS2 (FGRRES_05372) | 65 | <i>F. solani</i> f.sp. <i>pisi</i> (XP_003044019) | 91 |
| NRPS6 (Neo_004434) | NRPS6 (FGRRES_03747) | 78 | <i>F. solani</i> f.sp. <i>pisi</i> (XP_003043406) | 96 |
| NRPS27 (Neo_005330) | NRPS6 (FGRRES_03747) | 45 | <i>F. solani</i> f.sp. <i>pisi</i> (XP_003048492) | 94 |
| SimA (Neo_003447) | NRPS19 (FGRRES_15676) | 43 | <i>Tolypocladium inflatum</i> (CAA82227) | 96 |
| TC1 (Neo_002462) | ERG9 (FGRRES_09381) | 87 | <i>F. solani</i> f.sp. <i>pisi</i> (XP_003053888) | 98 |
| TC2 (Neo_003698) | TRI5 (FGRRES_03537) | 42 | <i>F. solani</i> f.sp. <i>pisi</i> (XP_003047531) | 90 |
| TC3 (Neo_003381) | – (FGRRES_16578) | 81 | <i>F. solani</i> f.sp. <i>pisi</i> (XP_003050574) | 96 |

^aAnnotations of PKS and NRPS genes, respectively, as in Hansen et al. (2015) and Brown and Proctor (2016). ^bPercent similarity of deduced polypeptides sequence. ^cBLASTp search results performed on November 16, 2018. Accessions are in parenthesis.

development. *PKS3*, *PKS30*, and *PKS33* were induced at earlier developmental stages and declined afterward. By comparison, expression of *PKS2*, *PKS7*, *PKS35*, and *TC2* peaked at later developmental stages.

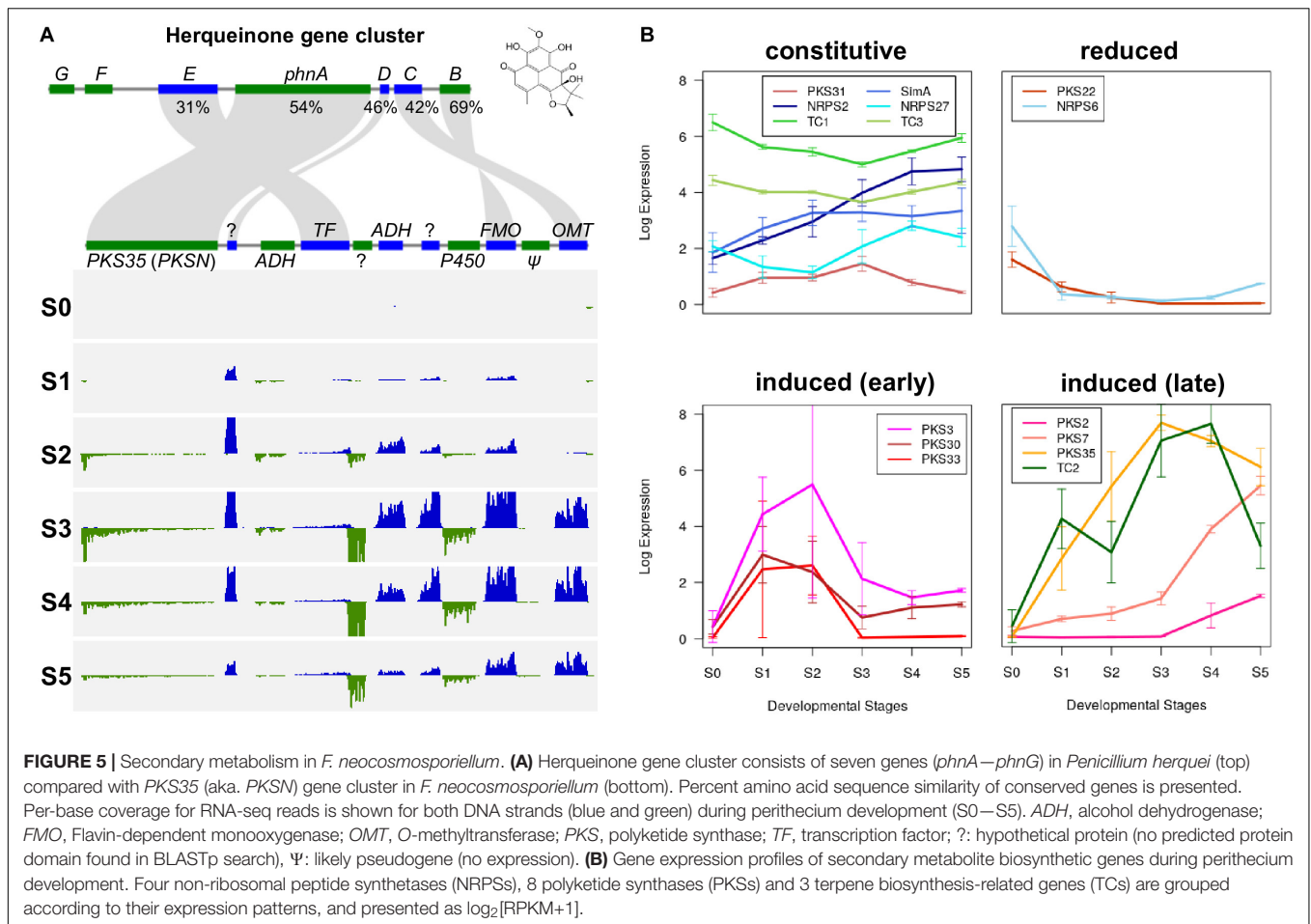
To determine whether SM genes have a role in perithecium development, we selected three *PKS7*, *PKS35*, and *TC2* for functional analysis by targeted gene deletion, which were highly induced at the later stages of development (Figure 5B). The metabolic products of *PKS7*- and *TC2*-encoded enzymes are not known, whereas the *PKS35*-encoded enzyme is required for production of a red perithecial pigment (Graziani et al., 2004). Deletion of *PKS35* did not cause any visible change in growth, asexual sporulation, or ascospore formation. However, perithecia produced by the Δ *PKS35* were albino, suggesting a specific role of *PKS35* in perithecial wall pigmentation in *F. neocosmosporiellum* (Figure 6). Deletion of *PKS7* caused aborted perithecium development, leading to production of smaller perithecia that were devoid of asci (Figure 6). This defective phenotype was restored by genetic complementation of the Δ *PKS7* with the wild-type copy of *PKS7* (Supplementary Figure S1). Deletion of *TC2* did not cause any detectable morphological differences (Figure 6).

DISCUSSION

We used a comparative genomic and transcriptomic approach to functionally analyze an organism whose life history remains unclear. Our study centered on the perithecium development, because fruiting bodies provide the primary long distance dispersal and long-term survival propagules, especially for ascomycetes fungi, and because *F. neocosmosporiellum* produces prolific perithecia in culture. Formation of sexual fruiting bodies is a crucial step in the life cycle of many fungi. It requires sensing of environmental cues to initiate

and complete development fruiting bodies and to disperse sexual spores produced within them. Fruiting body form and function is diverse, even among species in the genus *Fusarium*, and the diverse mechanisms have evolved that facilitate ascospore dispersal and survival. Perithecia of *F. neocosmosporiellum* and *F. graminearum* have distinct features, which may have ecological relevance. These features include: (1) production of round, single-celled ascospores, instead of ellipsoidal, multiseptate ascospores of many *Fusarium* spp. (Smith, 2007); (2) the majority of spores are released through cirrhi that are most likely splash-dispersed; and (3) perithecia are larger than those produced by *F. graminearum* (300 μ m in *F. neocosmosporiellum* compared with 180 μ m in *F. graminearum*) (Calaça et al., 2013; Gabriel et al., 2013; Sun et al., 2014).

Ellipsoidal ascospores that are forcibly discharged are prevalent throughout the Ascomycota and in most perithecium-producing *Fusarium* species (Zhou et al., 2018). This shape is optimized for low drag (Roper et al., 2008). However, those produced by *F. neocosmosporiellum* are globose-to-subglobose, which may be explained by the loss of the ability to produce septate ascospores (O'Donnell, 2000). We have shown that the majority of the ascospores produced by *F. neocosmosporiellum* are not forcibly discharged; instead they accumulate in a cirrhous. From the pattern of deposition of spores forcibly discharged, we can infer that ascospores remain attached after they are discharged, and that they are likely held together by a mucilaginous droplet during flight. Production of a large, multi-ascospore projectile could overcome air drag that would be effective on a single spore, due to a larger projectile force from the increased mass. In *F. graminearum*, by contrast, ascospores disperse from each other after they are forcibly discharged from perithecia. In addition, ascospores discharged from *F. graminearum* perithecia are not coated in mucilage, as they are in *F. neocosmosporiellum*. As a result, when dispersed onto a glass surface, *F. graminearum*



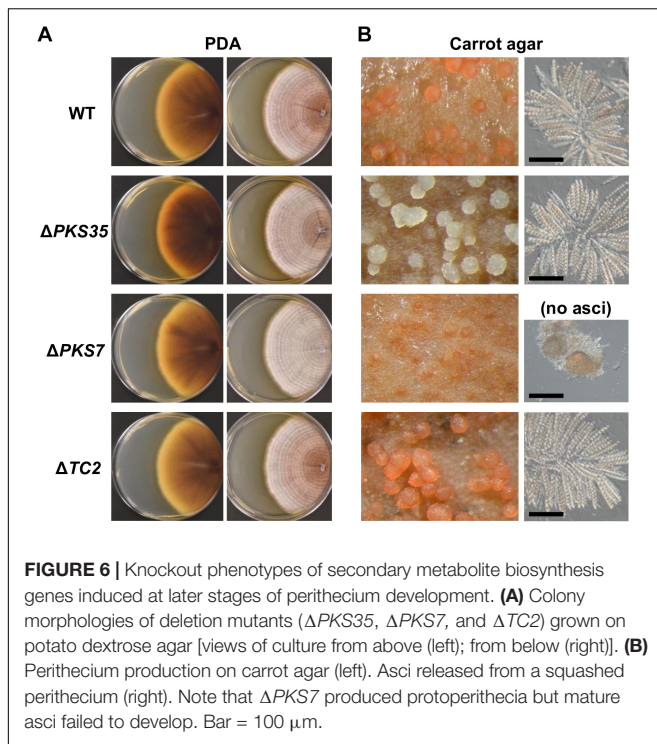
ascospores are easily washed off (Trail et al., 2005), whereas *F. neocosmosporiellum* are not.

We have shown that *F. graminearum* spores are launched an average of 0.6 cm in the chamber we used in this study (Trail et al., 2005). A group of reports summarized by Calaça et al. (2013) indicate *F. neocosmosporiellum* is a coprophilous fungus based on its recovery from a variety of herbivore dung in Africa, Italy and Brazil. *Coprophilous ascomycetes* fungi often share several characteristics (Krug et al., 2004). They tend to discharge large projectiles that are capable of escaping the “zone of repugnance” where some spores by chance land on vegetation and may be ingested by herbivore. The ascospores of *F. neocosmosporiellum* have unusually thick walls (Calaça et al., 2013), which may serve as protection against the harsh environment of a herbivore gut. In addition, the presence of larger numbers of lysozyme genes (GH24 and GH25 families) that we found in the genome of *F. neocosmosporiellum* might enhance its competitiveness on dung.

The level of *MAT* gene expression appears to be correlated with fertility in *F. graminearum* (Kim et al., 2012). Interestingly, three strains of the closely related species, *F. asiaticum*, which is also a member of the FSAMSC, exhibited lower fertility, and their *MAT* gene expression levels were significantly lower than *F. graminearum* (Kim et al., 2012). *Fusarium*

neocosmosporiellum NRRL 22166 is highly fertile. All five *MAT* genes are highly induced in a coordinated manner, producing abundant perithecia on diverse agar media, including PDA, on which *F. graminearum* does not produce perithecia. The observed difference in *MAT* gene expression patterns between the two fusaria suggests different regulatory networks, including those for *MAT* genes during perithecium development. The plant pathogen *F. graminearum* discharges ascospores when the temperature is warmer, which coincides when hosts are available (Guenther and Trail, 2005). Additionally, *F. graminearum* can produce perithecia in association with specific host cells (Guenther and Trail, 2005). The timing and location of perithecium production by *F. neocosmosporiellum* in nature are not known; however, our findings suggest that they may accommodate variable conditions.

CAZymes are essential components of fungal cells because they facilitate absorptive nutrition. Coordination of a set of CAZymes is required to liberate monomeric sugars from plant biomass, along with accessory enzymes that cleave side chains of poly- and oligosaccharides. We found that sets of co-expressed CAZyme genes were induced in different stages of perithecium development, indicating that they appear to act cooperatively and play stage-specific developmental roles in *F. graminearum* and *F. neocosmosporiellum*. The type of CAZymes encoded in fungal



genomes and their expression at different stages of the life cycle are potential clues to the nutrient sources they require. Recent comparative genomic analyzes revealed that carbon utilization is not correlated with CAZyme content in the aspergilli (Vesth et al., 2018). The authors suggested that differences in their ability to degrade plant biomass is reflected by the level of CAZymes gene expression rather than copy number. Although CAZyme content was largely conserved between *F. graminearum* and *F. neocosmosporiellum*, some CAZyme families showed different copy numbers and divergent expression patterns in the latter species. We discovered several CAZyme families in *F. neocosmosporiellum* that offered clues to its ecology. These included CAZymes that targeted plant cell wall components, such as cellulose and pectin, and lysozymes targeting bacterial cells. Collectively, these enzymes suggest that *F. neocosmosporiellum* is well adapted to life as a saprotroph, soil-dwelling, coprophile, and weak phytopathogen.

The plant pathogen *F. graminearum* colonizes host plants by penetrating intercellular spaces rich in pectin (Jansen et al., 2005) and produces perithecia on host tissues after the host has senesced (Trail, 2009). The three putative pectin acetylsterases (CAZyme family CE12) involved in pectin degradation were highly induced during the early developmental stage on carrot agar medium, suggesting that *F. graminearum* may be more efficient at using pectin as a carbon source in this earlier stage. By way of comparison, *F. neocosmosporiellum* appears to have lost some of the CAZyme families related to degradation of plant biomass, such as hemicellulose and cutin (CAZyme family CE5). Loss of cutinases may indicate a change in the mode of pathogenicity, although the role for cutinase in virulence of *F. solani* f. sp. *pisi* on garden

pea has been controversial (Stahl and Schafer, 1992; Rogers et al., 1994; Stahl et al., 1994). However, in *Magnaporthe grisea* mutation of the Cutinase2 gene (*CUT2*) attenuated virulence (Skamnioti and Gurr, 2007, 2008). *F. neocosmosporiellum* possesses three cellulases (CAZyme family GH5), compared with only one in *F. graminearum*, and two of them are induced at early or late developmental stages. In addition, genes for three lysozymes were found in *F. neocosmosporiellum*, targeting bacterial cell walls (i.e., peptidoglycan), which are absent in *F. graminearum*. Among them, Neo_008641 (GH25) has not been reported in other *Fusarium* species. These enzymes might facilitate survival in the ecological niches that *F. neocosmosporiellum* occupies, supporting a predominantly saprotrophic lifestyle.

Divergence of the transport-related gene repertoire has contributed to evolution of fungal fruiting bodies (Nguyen et al., 2017). *F. neocosmosporiellum* NRRL 22166 possesses more nutrient transport-related genes than *F. graminearum* PH-1, and the transcriptome data shows that many of these genes in the former species are specifically induced between S2 and S3. This observation suggested that *F. neocosmosporiellum* may require active transport of carbon and other nutrients, which may account for the large increase in perithecium volume in a relatively short time period. Interestingly, a *F. graminearum* knockout mutant lacking a MYB-family transcription factor gene produces larger perithecia that were approximately the same size as those of *F. neocosmosporiellum* (Lin et al., 2012). In eukaryotes, MYB-family proteins are involved in cell proliferation and differentiation (Oh and Reddy, 1999). In our transcriptome data, expression of the *MYT2* ortholog in *F. neocosmosporiellum* was high at S1, decreased at S2, but was high again at S3. However, expression of *MYT2* in *F. graminearum* remained high from S1 through S3 (data not shown). These expression patterns suggest that *MYT2* might function as a negative regulator of cell proliferation during perithecium development, presumably by controlling nutrient transport-related genes. Furthermore, the decreased expression level of the *MYT2* ortholog at S2 may explain why *F. neocosmosporiellum* produces perithecia that are larger than in *F. graminearum*. To test this hypothesis, we attempted to generate *MYT2*-deletion mutants in *F. neocosmosporiellum*. However, several unsuccessful attempts to obtain the mutant suggests that the *MYT2* ortholog in *F. neocosmosporiellum* is essential.

Secondary metabolites are often implicated in niche adaptation and host specialization especially for pathogens or parasites (Turgeon and Bushley, 2010). Various fungi within the Hypocreales, including *F. neocosmosporiellum*, have been reported to produce cyclosporines, which are used as immunosuppressant drugs (Borel et al., 1977). Here, we identified a full-length cyclosporine synthetase gene, *SimA* (45,825 bp-long), for the first time in the Nectriaceae. Cyclosporines are produced by many insect parasites, such as *Beauveria* spp. and *Tolyocladium inflatum*, and are important virulence factors against susceptible insect hosts (Yang et al., 2018). Though presently unknown, frequent isolation of *F. neocosmosporiellum* from soybean cyst nematodes may be due to the toxic properties of cyclosporines (Gintis et al., 1983).

Orthologs of *F. neocosmosporiellum* PKS genes are present in other members of the FSSC, including *F. solani* f. sp. *pisi* and *F. euwallaceae* (80–95% AA sequence similarity). Of these, *PKS7* exhibited the least sequence identity (80%) among FSSC members and appears to be fast-evolving. Despite the sequence divergence, the protein sequence and domain structure of *PKS7* in *F. neocosmosporiellum* is conserved with the orthologous gene in *F. graminearum*. Interestingly, a deletion mutant of *PKS7* in *F. graminearum* also failed to develop mature perithecia, suggesting a conserved function of the yet-unknown PKS products in perithecium development (Kim H.-K. et al., 2015). We are currently trying to determine the metabolic product(s) of the *PKS7* gene cluster and its role in perithecium development.

The results of our study demonstrate that *PKS35* is required for the red pigmentation of *F. neocosmosporiellum*, as has been reported previously for another member of the FSSC (Graziani et al., 2004). Our analysis also revealed that the *PKS35* cluster includes a flavin-dependent monooxygenase gene with 69% deduced AA sequence identity to PhnB, the enzyme catalyzes the final step in biosynthesis of the red pigment herquinone. This final step is essential for formation of the three-ring phenalenone structure that makes up a large part of the herquinone molecule. In addition, the domain structure of *PKS35* and the herquinone PKS, PhnA, are nearly identical. These observations suggest that the two red pigments, one that accumulates in the perithecial wall of *F. neocosmosporiellum* and the other secreted by hyphae of *Penicillium herquei*, might share a common evolutionary origin and core chemical structure. In addition, *PKS35* orthologs have been reported in several members of the FSSC (Hansen et al., 2015; Brown and Proctor, 2016). Although red pigments produced by land plants are thought to attract insects (Tanaka et al., 2008), future studies are needed to determine whether those produced in the perithecia of *F. neocosmosporiellum* have a similar function.

Throughout the last century, much emphasis has been placed on the study of life histories of disease-causing plant pathogens. More recently, scientists have combined molecular genetics and genomics tools to identify specific genes involved in pathogenicity. Here, we have used a comparative genomic and transcriptomic approach to provide a functional view of perithecium development and to identify biological clues into the life history of *F. neocosmosporiellum*, a cosmopolitan fungus that has been found in a variety of niches, including dung

and soil. Furthermore, *F. neocosmosporiellum* ascospores have morphological characteristics that are similar to other dung fungi. In summary, this study revealed transcriptional programming that accompanied production of large perithecia and secondary metabolites linked to perithecium development, processes that may facilitate survival and dispersal of this cosmopolitan fungus in nature.

AUTHOR CONTRIBUTIONS

WK and FT conceived and designed the experiments. WK and FT performed the experiments. KO and RP sequenced the genome. BC annotated the genome. WK and FT analyzed the data and wrote the manuscript. JT, KO, and RP edited the manuscript. FT and JT conceived of the larger project which includes this study, and obtained the funding.

FUNDING

This publication is based upon work supported by the National Science Foundation under Grant Number (1456482 to FT; IOS-1457044 to JT) and Michigan AgBioResearch (to FT). The funders had no role in study design, data collection and analysis, decision to publish, or preparation of the manuscript.

ACKNOWLEDGMENTS

We thank Gail Doehring (USDA, Peoria, IL, United States) for analysis of the *MAT* loci in *Fusarium neocosmosporiellum*, Amy McGovern and Crystal Probyn for generation of genome sequences, and Kevin Childs (Michigan State University) for providing Perl scripts to produce **Figure 3A**. We also thank Tara Watkins for constructive comments during the revision process and Megan Burgess for technical assistance.

SUPPLEMENTARY MATERIAL

The Supplementary Material for this article can be found online at: <https://www.frontiersin.org/articles/10.3389/fmicb.2019.01247/full#supplementary-material>

REFERENCES

- Anders, S., Pyl, P. T., and Huber, W. (2015). HTSeq—a Python framework to work with high-throughput sequencing data. *Bioinformatics* 31, 166–169. doi: 10.1093/bioinformatics/btu638
- Aylor, D. E., and Anagnostakis, S. L. (1991). Active discharge distance of ascospores of *Venturia inaequalis*. *Phytopathology* 81, 548–551.
- Borel, J. F., Feurer, C., Magnée, C., and Stähelin, H. (1977). Effects of the new anti-lymphocytic peptide cyclosporin A in animals. *Immunology* 32, 1017–1025.
- Brown, D. W., and Proctor, R. H. (2016). Insights into natural products biosynthesis from analysis of 490 polyketide synthases from *Fusarium*. *Fungal Genet. Biol.* 89, 37–51. doi: 10.1016/j.fgb.2016.01.008
- Bryant, D. M., Johnson, K., DiTommaso, T., Tickle, T., Couger, M. B., Payzin-Dogru, D., et al. (2017). A tissue-mapped axolotl de novo transcriptome enables identification of limb regeneration factors. *Cell. Rep.* 18, 762–776. doi: 10.1016/j.celrep.2016.12.063
- Budd, K. (1969). The assimilation of bicarbonate by *Neocosmospora vasinfecta*. *Can. J. Microbiol.* 15, 389–398. doi: 10.1139/m69-070
- Bushley, K. E., Raja, R., Jaiswal, P., Cumbie, J. S., Nonogaki, M., Boyd, A. E., et al. (2013). The genome of *Tolypocladium inflatum*: evolution, organization, and expression of the cyclosporin biosynthetic gene cluster. *PLoS Genet.* 9:e1003496. doi: 10.1371/journal.pgen.1003496
- Calaça, F., Silva, N., Hirooka, Y., and Xavier-Santos, S. (2013). *Neocosmospora vasinfecta* (Nectriaceae): a new record as a fimicolous ascomycota from Brazil. *Mycosphere* 4, 999–1004.

- Cappellini, R. A., and Peterson, J. L. (1965). Macroconidium formation in submerged cultures by a non-sporulating strain of *Gibberella zeae*. *Mycologia* 57, 962–966. doi: 10.2307/3756895
- Carroll, A. M., Sweigard, J. A., and Valent, B. (1994). Improved vectors for selecting resistance to hygromycin. *Fungal Genet. Newsl.* 41:22. doi: 10.4148/1941-4765.1367
- Catlett, N. L., Lee, B., Yoder, O. C., and Turgeon, B. C. (2003). Split-marker recombination for efficient targeted deletion of fungal genes. *Fungal Genet. Newsl.* 50, 9–11. doi: 10.4148/1941-4765.1150
- Chen, C., Khaleel, S. S., Huang, H., and Wu, C. H. (2014). Software for pre-processing Illumina next-generation sequencing short read sequences. *Source Code Biol. Med.* 9:8. doi: 10.1186/1751-0473-9-8
- Coleman, J. J., Rounsley, S. D., Rodriguez-Carres, M., Kuo, A., Wasmann, C. C., Grimwood, J., et al. (2009). The genome of *Nectria haematococca*: contribution of supernumerary chromosomes to gene expansion. *PLoS Genet.* 5:e1000618. doi: 10.1371/journal.pgen.1000618
- Cornely, O. A., Chemnitz, J., Brochhagen, H.-G., Lemmer, K., Schütt, H., Söhngen, D., et al. (2001). Disseminated *Neocosmospora vasinfecta* infection in a patient with acute nonlymphocytic leukemia. *Emerg. Infect. Dis.* 7, 149–152. doi: 10.3201/eid0701.010123
- Dau, V. T., Pham, L. T., Luong, T. M., Huynh, L. M. T., Tran, N. T., Ho, T. D., et al. (2010). First report of *Neocosmospora vasinfecta* associated with the root rot complex of peanuts in Vietnam. *Australas. Plant Dis. Notes* 5, 79–81. doi: 10.1071/DN10028
- Desjardins, A. E., Plattner, R. D., Shaner, G., Brown, D. W., Buechley, G., Proctor, R. H., et al. (2006). “Field release of *Gibberella zeae* genetically modified to lack ascospores,” in *Fusarium Head Blight Forum*, eds S. M. Canty, A. Clark, and V. D. Sanford (Lexington, KY: University of Kentucky), 39–44.
- Eddy, S. R. (2011). Accelerated profile HMM searches. *PLoS Comput. Biol.* 7:e1002195. doi: 10.1371/journal.pcbi.1002195
- Frandsen, R. J. N., Rasmussen, S. A., Knudsen, P. B., Uhlig, S., Petersen, D., Lysoe, E., et al. (2016). Black perithecial pigmentation in *Fusarium* species is due to the accumulation of 5-deoxybostrycoidin-based melanin. *Sci. Rep.* 6:26206. doi: 10.1038/srep26206
- Gabriel, F., D’Almeida, M., Albert, O., Fitton-Ouhabi, V., Noël, T., and Accocceberry, I. (2013). A disseminated infection with the antifungal-multiresistant teleomorph fungus *Neocosmospora vasinfecta* in a patient with acute B-lymphoblastic leukemia. *Med. Mycol. Case. Rep.* 2, 44–47. doi: 10.1016/j.mmcr.2013.01.004
- Gaffoor, I., Brown, D. W., Plattner, R., Proctor, R. H., Qi, W., and Trail, F. (2005). Functional analysis of the polyketide synthase genes in the filamentous fungus *Gibberella zeae* (Anamorph *Fusarium graminearum*). *Eukaryot. Cell* 4, 1926–1933. doi: 10.1128/EC.4.11.1926-1933.2005
- Gao, S.-S., Duan, A., Xu, W., Yu, P., Hang, L., Houk, K. N., et al. (2016). Phenalenone polyketide cyclization catalyzed by fungal polyketide synthase and flavin-dependent monooxygenase. *J. Am. Chem. Soc.* 138, 4249–4259. doi: 10.1021/jacs.6b01528
- Geiser, D. M., Aoki, T., Bacon, C. W., Baker, S. E., Bhattacharyya, M. K., Brandt, M. E., et al. (2013). One fungus, one name: defining the genus *Fusarium* in a scientifically robust way that preserves longstanding use. *Phytopathology* 103, 400–408. doi: 10.1094/PHYTO-07-12-0150-LE
- Gintis, B. O., Morgan-Jones, G., and Rodriguez-Kabana, R. (1983). Fungi associated with several developmental stages of *Heterodera glycines* from an Alabama soybean field soil. *Nematropica* 13, 181–200.
- Graziani, S., Vasnier, C., and Daboussi, M.-J. (2004). Novel polyketide synthase from *Nectria haematococca*. *Appl. Environ. Microbiol.* 70, 2984–2988. doi: 10.1128/AEM.70.5.2984-2988.2004
- Greer, A. M., Spurlock, T. N., and Coker, C. M. (2015). First report of *Neocosmospora* stem rot of soybean caused by *Neocosmospora vasinfecta* in Arkansas. *Plant Dis.* 99:554. doi: 10.1094/pdis-05-14-0559-pdn
- Gruninger, R. J., Nguyen, T. T. M., Reid, I. D., Yanke, J. L., Wang, P., Abbott, D. W., et al. (2018). Application of transcriptomics to compare the carbohydrate active enzymes that are expressed by diverse genera of anaerobic fungi to degrade plant cell wall carbohydrates. *Front. Microbiol.* 9:1581. doi: 10.3389/fmicb.2018.01581
- Guenther, J. C., and Trail, F. (2005). The development and differentiation of *Gibberella zeae* (anamorph: *Fusarium graminearum*) during colonization of wheat. *Mycologia* 97, 229–237. doi: 10.1080/15572536.2006.11832856
- Hallen-Adams, H. E., Cavinder, B. L., and Trail, F. (2011). “*Fusarium graminearum* from expression analysis to functional assays,” in *Fungal Genomics, part of the Methods in Molecular Biology book series*, eds J. R. Xu and B. Bluhm (New York: Humana Press), 79–101. doi: 10.1007/978-1-61779-040-9_6
- Hansen, F. T., Gardiner, D. M., Lysoe, E., Fuentes, P. R., Tudzynski, B., Wiemann, P., et al. (2015). An update to polyketide synthase and non-ribosomal synthetase genes and nomenclature in *Fusarium*. *Fungal Genet. Biol.* 75, 20–29. doi: 10.1016/j.fgb.2014.12.004
- Holt, C., and Yandell, M. (2011). MAKER2: an annotation pipeline and genome-database management tool for second-generation genome projects. *BMC Bioinformatics* 12:491. doi: 10.1186/1471-2105-12-491
- Huang, L., Zhang, H., Wu, P., Entwistle, S., Li, X., Yohe, T., et al. (2018). dbCAN-seq: a database of carbohydrate-active enzyme (CAZyme) sequence and annotation. *Nucleic Acids Res.* 46, D516–D521. doi: 10.1093/nar/gkx894
- Hughes, T. J., O’Donnell, K., Sink, S., Rooney, A. P., Scandiani, M. M., Luque, A., et al. (2014). Genetic architecture and evolution of the mating type locus in *Fusaria* that cause soybean sudden death syndrome and bean root rot. *Mycologia* 106, 686–697. doi: 10.3852/13-318
- Jansen, C., Wettstein, D., von Schäfer, W., Kogel, K.-H., Felk, A., and Maier, F. J. (2005). Infection patterns in barley and wheat spikes inoculated with wild-type and trichodiene synthase gene disrupted *Fusarium graminearum*. *PNAS* 102, 16892–16897. doi: 10.1073/pnas.0508467102
- Kim, D., Langmead, B., and Salzberg, S. L. (2015). HISAT: a fast spliced aligner with low memory requirements. *Nat. Methods* 12, 357–360. doi: 10.1038/nmeth.3317
- Kim, H.-K., Jo, S.-M., Kim, G.-Y., Kim, D.-W., Kim, Y.-K., and Yun, S.-H. (2015). A large-scale functional analysis of putative target genes of mating-type loci provides insight into the regulation of sexual development of the cereal pathogen *Fusarium graminearum*. *PLoS Genet.* 11:e1005486. doi: 10.1371/journal.pgen.1005486
- Kim, H.-K., Cho, E. J., Lee, S., Lee, Y.-S., and Yun, S.-H. (2012). Functional analyses of individual mating-type transcripts at MAT loci in *Fusarium graminearum* and *Fusarium asiaticum*. *FEMS Microbiol. Lett.* 337, 89–96. doi: 10.1111/1574-6968.12012
- Kim, W., Miguel-Rojas, C., Wang, J., Townsend, J. P., and Trail, F. (2018). Developmental dynamics of long noncoding RNA expression during sexual fruiting body formation in *Fusarium graminearum*. *mBio* 9, e1292–e1218. doi: 10.1128/mBio.01292-1218
- King, R., Brown, N. A., Urban, M., and Hammond-Kosack, K. E. (2018). Inter-genome comparison of the Quorn fungus *Fusarium venenatum* and the closely related plant infecting pathogen *Fusarium graminearum*. *BMC Genomics* 19:269. doi: 10.1186/s12864-018-4612-4612
- King, R., Urban, M., Hammond-Kosack, M. C. U., Hassani-Pak, K., and Hammond-Kosack, K. E. (2015). The completed genome sequence of the pathogenic ascomycete fungus *Fusarium graminearum*. *BMC Genomics* 16:544. doi: 10.1186/s12864-015-1756-1751
- Klittich, C., and Leslie, J. F. (1988). Nitrate reduction mutants of *Fusarium moniliforme* (*Gibberella fujikuroi*). *Genetics* 118, 417–423.
- Krug, J. C., Benny, G. L., and Keller, H. W. (2004). “21 - coprophilous fungi,” in *Biodiversity of Fungi*, eds G. M. Mueller, G. F. Bills, and M. S. Foster (Burlington: Academic Press), 467–499. doi: 10.1016/b978-012509551-8/50024-6
- Langfelder, P., and Horvath, S. (2008). WGCNA: an R package for weighted correlation network analysis. *BMC Bioinformatics* 9:559. doi: 10.1186/1471-2105-9-559
- Law, C. W., Alhamdoosh, M., Su, S., Smyth, G. K., and Ritchie, M. E. (2016). RNA-seq analysis is easy as 1-2-3 with limma, Glimma and edgeR. *F1000Res.* 5:1408. doi: 10.12688/f1000research.9005.2
- Li, L., Stoeckert, C. J., and Roos, D. S. (2003). OrthoMCL: identification of ortholog groups for eukaryotic genomes. *Genome Res.* 13, 2178–2189. doi: 10.1101/gr.1224503
- Lin, Y., Son, H., Min, K., Lee, J., Choi, G. J., Kim, J.-C., et al. (2012). A putative transcription factor MYT2 regulates perithecial size in the ascomycete *Gibberella zeae*. *PLoS One* 7:e37859. doi: 10.1371/journal.pone.0037859
- Lombard, V., Golaconda Ramulu, H., Drula, E., Coutinho, P. M., and Henrissat, B. (2014). The carbohydrate-active enzymes database (CAZy) in 2013. *Nucleic Acids Res.* 42, D490–D495. doi: 10.1093/nar/gkt1178
- Medema, M. H., Blin, K., Cimermancic, P., de Jager, V., Zakrzewski, P., Fischbach, M. A., et al. (2011). antiSMASH: rapid identification, annotation and analysis of

- secondary metabolite biosynthesis gene clusters in bacterial and fungal genome sequences. *Nucleic Acids Res.* 39, W339–W346. doi: 10.1093/nar/gkr466
- Metzenberg, R. L., and Glass, N. L. (1990). Mating type and mating strategies in *Neurospora*. *Bioessays* 12, 53–59. doi: 10.1002/bies.950120202
- Nguyen, T. A., Cissé, O. H., Wong, J. Y., Zheng, P., Hewitt, D., Nowrousian, M., et al. (2017). Innovation and constraint leading to complex multicellularity in the Ascomycota. *Nat. Commun.* 8:14444. doi: 10.1038/ncomms14444
- O'Donnell, K. (2000). Molecular phylogeny of the *Nectria haematococca-Fusarium solani* species complex. *Mycologia* 92, 919–938. doi: 10.2307/3761588
- O'Donnell, K., Rooney, A. P., Proctor, R. H., Brown, D. W., McCormick, S. P., Ward, T. J., et al. (2013). Phylogenetic analyses of RPB1 and RPB2 support a middle Cretaceous origin for a clade comprising all agriculturally and medically important fusaria. *Fungal Genet. Biol.* 52, 20–31. doi: 10.1016/j.fgb.2012.12.004
- O'Donnell, K., Sutton, D. A., Rinaldi, M. G., Sarver, B. A. J., Balajee, S. A., Schroers, H.-J., et al. (2010). Internet-accessible DNA sequence database for identifying fusaria from human and animal infections. *J. Clin. Microbiol.* 48, 3708–3718. doi: 10.1128/JCM.00989-10
- Oh, I.-H., and Reddy, E. P. (1999). The myb gene family in cell growth, differentiation and apoptosis. *Oncogene* 18, 3017–3033. doi: 10.1038/sj.onc.1202839
- Pan, R., Deng, Q., Deng, M., Guan, M., Xu, D., Gai, Y., et al. (2010). First report of peanut foot rot caused by *Neocosmospora vasinfecta* in mainland China. *Plant Pathol.* 59, 1172–1172. doi: 10.1111/j.1365-3059.2010.02360.x
- Robinson, M. D., McCarthy, D. J., and Smyth, G. K. (2010). edgeR: a bioconductor package for differential expression analysis of digital gene expression data. *Bioinformatics* 26, 139–140. doi: 10.1093/bioinformatics/btp616
- Rodriguez, R. J. Jr., White, J. F., Arnold, A. E., and Redman, R. S. (2009). Fungal endophytes: diversity and functional roles. *New Phytol.* 182, 314–330. doi: 10.1111/j.1469-8137.2009.02773.x
- Rogers, L. M., Flaishman, M. A., and Kolattukudy, P. E. (1994). Cutinase gene disruption in *Fusarium solani* f sp pisi decreases its virulence on pea. *Plant Cell* 6, 935–945. doi: 10.1105/tpc.6.7.935
- Roper, M., Pepper, R. E., Brenner, M. P., and Pringle, A. (2008). Explosively launched spores of ascomycete fungi have drag-minimizing shapes. *PNAS* 105, 20583–20588. doi: 10.1073/pnas.0805017105
- Sikhakolli, U. R., López-Giráldez, F., Li, N., Common, R., Townsend, J. P., and Trail, F. (2012). Transcriptome analyses during fruiting body formation in *Fusarium graminearum* and *Fusarium verticillioides* reflect species life history and ecology. *Fungal Genet. Biol.* 49, 663–673. doi: 10.1016/j.fgb.2012.05.009
- Simão, F. A., Waterhouse, R. M., Ioannidis, P., Kriventseva, E. V., and Zdobnov, E. M. (2015). BUSCO: assessing genome assembly and annotation completeness with single-copy orthologs. *Bioinformatics* 31, 3210–3212. doi: 10.1093/bioinformatics/btv351
- Skamnioti, P., and Gurr, S. J. (2007). *Magnaporthe grisea* cutinase2 mediates appressorium differentiation and host penetration and is required for full virulence. *Plant Cell* 19, 2674–2689. doi: 10.1105/tpc.107.051219
- Skamnioti, P., and Gurr, S. J. (2008). Cutinase and hydrophobin interplay: a herald for pathogenesis?. *Plant Signal. Behav.* 3, 248–250. doi: 10.4161/psb.3.4.5181
- Smith, S. N. (2007). An overview of ecological and habitat aspects in the genus *Fusarium* with special emphasis on the soil-borne pathogenic forms. *Plant Pathol. Bull.* 16, 97–120.
- Son, H., Seo, Y.-S., Min, K., Park, A. R., Lee, J., Jin, J.-M., et al. (2011). A phenome-based functional analysis of transcription factors in the cereal head blight fungus, *Fusarium graminearum*. *PLoS Pathog* 7:e1002310. doi: 10.1371/journal.ppat.1002310
- Stahl, D. J., and Schafer, W. (1992). Cutinase is not required for fungal pathogenicity on pea. *Plant Cell* 4, 1621–1629.
- Stahl, D. J., Theuerkauf, A., Heitefuss, R., and Schafer, W. (1994). Cutinase of *Nectria haematococca* (*Fusarium solani* F.sp. pisi) is not required for fungal virulence or organ specificity on pea. *Mol. Plant Microb. Interact.* 7, 713–725.
- Stodola, F. H., Raper, K. B., and Fennell, D. I. (1951). Pigments of *Penicillium herquei*. *Nature* 167, 773–774. doi: 10.1038/167773a0
- Sun, S. L., Kim, M. Y., Van, K., Lee, Y.-H., Zhong, C., Zhu, Z. D., et al. (2014). First report of *Neocosmospora vasinfecta* var. *vasinfecta* causing soybean stem rot in South Korea. *Plant Dis.* 98, 1744. doi: 10.1094/PDIS-06-14-0637-PDN
- Tanaka, Y., Sasaki, N., and Ohmiya, A. (2008). Biosynthesis of plant pigments: anthocyanins, betalains and carotenoids. *Plant J.* 54, 733–749. doi: 10.1111/j.1365-313X.2008.03447.x
- Teichert, I., Wolff, G., Kück, U., and Nowrousian, M. (2012). Combining laser microdissection and RNA-seq to chart the transcriptional landscape of fungal development. *BMC Genomics* 13:511. doi: 10.1186/1471-2164-13-511
- Trail, F. (2007). Fungal cannons: explosive spore discharge in the Ascomycota. *FEMS Microbiol. Lett.* 276, 12–18. doi: 10.1111/j.1574-6968.2007.00900.x
- Trail, F. (2009). For bighted waves of grain: *Fusarium graminearum* in the postgenomics era. *Plant Physiol.* 149, 103–110. doi: 10.1104/pp.108.129684
- Trail, F., Gaffoor, I., and Vogel, S. (2005). Ejection mechanics and trajectory of the ascospores of *Gibberella zeae* (anamorph *Fusarium graminearum*). *Fungal Genet. Biol.* 42, 528–533. doi: 10.1016/j.fgb.2005.03.008
- Trail, F., and Gardiner, D. M. (2014). “Application of genomics to the study of pathogenicity and development in *Fusarium*,” in *The Mycota: a comprehensive Treatise on Fungi as Experimental Systems for Basic and Applied Research*, eds M. Nowrousian and K. Esser (Berlin: Springer), 267–300. doi: 10.1007/978-3-642-45218-5_11
- Trail, F., Wang, Z., Stefanko, K., Cubba, C., and Townsend, J. P. (2017). The ancestral levels of transcription and the evolution of sexual phenotypes in filamentous fungi. *PLoS Genet.* 13:e1006867. doi: 10.1371/journal.pgen.1006867
- Turgeon, B. G., and Bushley, E. K. (2010). “Secondary metabolism,” in *Cellular and Molecular Biology of Filamentous Fungi*, eds K. A. Borkovich and D. J. Ebbole (Washington, DC: ASM press), 376–395.
- Vesth, T. C., Nybo, J. L., Theobald, S., Frisvad, J. C., Larsen, T. O., Nielsen, K. F., et al. (2018). Investigation of inter- and intraspecies variation through genome sequencing of *Aspergillus* section *Nigri*. *Nat. Genet.* 50, 1688–1695. doi: 10.1038/s41588-018-0246-241
- Wang, Z., Gudibanda, A., Ugwuowo, U., Trail, F., and Townsend, J. P. (2018). Using evolutionary genomics, transcriptomics, and systems biology to reveal gene networks underlying fungal development. *Fungal Biol. Rev.* 32, 249–264. doi: 10.1016/j.fbr.2018.02.001
- Wang, Z., Lehr, N., Trail, F., and Townsend, J. P. (2012). Differential impact of nutrition on developmental and metabolic gene expression during fruiting body development in *Neurospora crassa*. *Fungal Genet. Biol.* 49, 405–413. doi: 10.1016/j.fgb.2012.03.004
- Yang, X., Feng, P., Yin, Y., Bushley, K., Spatafora, J. W., and Wang, C. (2018). Cyclosporine biosynthesis in *Tolyocladium inflatum* benefits fungal adaptation to the environment. *mBio* 9, e1211–e1218. doi: 10.1128/mBio.01211-1218
- Young, M. D., Wakefield, M. J., Smyth, G. K., and Oshlack, A. (2010). Gene ontology analysis for RNA-seq: accounting for selection bias. *Genome Biol.* 11:R14. doi: 10.1186/gb-2010-11-2-r14
- Yu, J.-H., Hamari, Z., Han, K.-H., Seo, J.-A., Reyes-Domínguez, Y., and Scazzocchio, C. (2004). Double-joint PCR: a PCR-based molecular tool for gene manipulations in filamentous fungi. *Fungal Genet. Biol.* 41, 973–981. doi: 10.1016/j.fgb.2004.08.001
- Zhao, Z., Liu, H., Wang, C., and Xu, J.-R. (2013). Comparative analysis of fungal genomes reveals different plant cell wall degrading capacity in fungi. *BMC Genomics* 14:274. doi: 10.1186/1471-2164-14-274
- Zhou, X., O'Donnell, K., Kim, H.-S., Proctor, R. H., Doehring, G., and Cao, Z.-M. (2018). Heterothallic sexual reproduction in three canker-inducing tree pathogens within the *Fusarium torreyae* species complex. *Mycologia* 110, 710–725. doi: 10.1080/00275514.2018.1491766

Conflict of Interest Statement: The authors declare that the research was conducted in the absence of any commercial or financial relationships that could be construed as a potential conflict of interest.

Copyright © 2019 Kim, Cavinder, Proctor, O'Donnell, Townsend and Trail. This is an open-access article distributed under the terms of the Creative Commons Attribution License (CC BY). The use, distribution or reproduction in other forums is permitted, provided the original author(s) and the copyright owner(s) are credited and that the original publication in this journal is cited, in accordance with accepted academic practice. No use, distribution or reproduction is permitted which does not comply with these terms.